X-ray and optical characterization of β-$FeSi_2$ layers formed by pulsed ion-beam treatment



2001 J. Phys.: Condens. Matter 13 L113

(http://iopscience.iop.org/0953-8984/13/5/101)

INSTITUTE OF PHYSICS PUBLISHING JOURNAL OF PHYSICS: CONDENSED MATTER

J. Phys.: Condens. Matter **13** (2001) L113–L118 www.iop.org/Journals/cm PII: S0953-8984(01)19615-3

**LETTER TO THE EDITOR**

# X-ray and optical characterization of $\beta$-$FeSi_2$ layers formed by pulsed ion-beam treatment

**R M Bayazitov and R I Batalov**

Kazan Physical-Technical Institute of RAS, Sibirsky Trakt 10/7, 420029 Kazan, Russia

E-mail: bayaz@kfti.knc.ru (R M Bayazitov)

Received 29 November 2000, in final form 11 January 2001

**Abstract**

$\beta$-$FeSi_2$ layers were formed on Si by means of high-dose $Fe^+$ implantation into Si(100) at 300 K followed by nanosecond pulsed ion-beam treatment (PIBT) of the implanted layers. It is shown that PIBT leads to the formation of a mixture of two phases (FeSi and $\beta$-$FeSi_2$) with a strained state of the silicide crystal lattice. Subsequent short-duration thermal annealing at 800 °C for 20 min results in a decrease of the lattice strains and in the complete transformation of the FeSi phase into the $\beta$-$FeSi_2$ phase, with the production of a highly textured layer with the [110] orientation. The results of the optical absorption measurements indicate the formation of a direct band gap structure with the optical gap $E_g \sim 0.83$ eV and the Urbach tail width $E_0 \sim 0.22$ eV.

## 1. Introduction

Formation of Si-based structures emitting in the visible and near-infrared (IR) spectral region has attracted substantial interest for the last 10–15 years. One of the main approaches to the fabrication of structures emitting at wavelengths $\lambda \sim 1.55$ $\mu$m is that of forming $\beta$-$FeSi_2$ layers. $\beta$-$FeSi_2$ is the semiconducting phase of the Fe–Si system, with orthorhombic structure and a direct band gap $E_g \sim 0.85$ eV [1–6]. This gap value corresponds to the optical wavelength $\lambda \sim 1.45$ $\mu$m which is close to the technologically important wavelength $\lambda \sim 1.55$ $\mu$m corresponding to the silicon transparency region and the absorption minimum of silica optical fibres. This allows one to create optoelectronic devices in the near-IR region integrated in silicon microelectronic device technology.

In order to form $\beta$-$FeSi_2$ layers, an ion-beam synthesis technique, i.e. high-dose $Fe^+$ implantation into Si with *in situ* heating [7, 8] or high-temperature and long-duration annealing ($T = 800$–$900$ °C, $t \sim 20$ h) [9–13], is widely used. However, during such thermal annealing a substantial degree of diffusion of iron atoms in the basic material takes place due to the large diffusion coefficient of Fe in Si at high temperatures ($D \sim 5 \times 10^{-6}$ cm$^2$ s$^{-1}$ at $T = 1000$ °C [14]). This can give rise to severe device yield and reliability problems [15].

Using nanosecond pulsed treatments by laser, electron and ion beams allows one to overcome this drawback by achieving local ($\sim$1 $\mu$m) and short-duration ($<$1 $\mu$s) heating

  

of the material. There have been many publications on pulsed-laser treatment of thin metal films on Si [16, 17]. However, they are all concerned with the formation of metal silicides for interconnections and ohmic and Schottky barrier contacts.

In order to synthesize semiconducting silicide $\beta$-$FeSi_2$ for optoelectronic applications, laser treatment of Fe films on Si is used [18], but there have been no reports on pulsed treatment of $Fe^+$-implanted Si. In this work, for the first time pulsed ion-beam treatment (PIBT) of $Fe^+$-implanted Si is used to form submicron $\beta$-$FeSi_2$ layers. A characteristic feature of PIBT is a more uniform depth distribution of energy losses in the material compared to that obtained under laser treatment, resulting in less surface overheating and disruption [19]. High rates of heating, melting and recrystallization ($\sim 10^7$–$10^9$ K $s^{-1}$) lead to the formation of epitaxial, defect-free and highly doped Si layers [20–22].

## 2. Experimental procedure

Single-crystal (100) Cz-Si wafers with an n-type resistivity of 1–4 Ω cm were implanted with $Fe^+$ ions at room temperature (RT) at an energy of 40 keV and dose of $1.8 \times 10^{17}$ $cm^{-2}$ (with an ion current density of 5 $\mu$A $cm^{-2}$). After the implantation, some of the implanted samples were subjected to PIBT using a TEMP accelerator [23] ($C^+$: 80%; $H^+$: 20%; $E = 300$ keV; $\tau = 50$ ns; $j \sim 50$ A $cm^{-2}$; $W \sim 0.75$ J $cm^{-2}$) with the total dose per pulse not exceeding $10^{14}$ $cm^{-2}$. The rest of the implanted samples were subjected to thermal annealing (TA) in a quartz furnace with ambient nitrogen at 800 °C for 20 min, to produce results for comparison. The crystal structure of the layers formed was studied by the glancing-x-ray diffraction technique (GXRD) using Fe K$\alpha$ radiation ($\lambda = 1.9373$ Å). The azimuth dependencies of the most intense diffraction peaks were measured by fixing the detector at the appropriate positions and performing azimuth angle scans from 0° to 360° with a step of 3°. IR spectroscopy in the reflection and transmission modes was employed to determine the band-gap energy. The measurements were performed at RT over the spectral range $\lambda = 1100$–$2000$ nm.

## 3. Results and discussion

### *3.1. X-ray characterization*

After ion implantation, no reflections are present in the GXRD pattern (not shown), indicating that complete amorphization of the implanted layer has taken place. Figure 1 shows GXRD patterns of samples subjected to various treatment regimes after ion implantation. From figure 1(a) one can see that after PIBT two phases are mixed: the metallic FeSi and the semiconducting $\beta$-$FeSi_2$. The most intense peak in the spectrum corresponds to the Bragg reflections from the (220)/(202) planes of the $\beta$-$FeSi_2$ phase. The position of this peak ($2\theta = 36.2°$) differs from the table value ($2\theta = 36.9°$). The disilicide crystal lattice deformation estimated from the difference between the interplane distances in the strained and unstrained states is $\varepsilon \sim 2\%$. Similar behaviour for other diffraction peaks present in the spectrum is observed. The difference observed in the positions of Bragg reflections can be explained by a strained state of the silicide crystal lattice, which is caused by the rapid liquid-phase crystallization after the PIBT.

In order to remove the lattice strains and to transform the residual FeSi phase into $\beta$-$FeSi_2$, a short-duration TA (800 °C, 20 min) was performed. The GXRD pattern after the additional TA is shown in figure 1(b). One can see a substantial increase of (220)/(202) $\beta$-$FeSi_2$ peak intensity and its shift to the value $2\theta = 36.9°$, indicating that the strains in the silicide lattice have been removed. Moreover, the Bragg reflections of the FeSi phase disappear as well. The

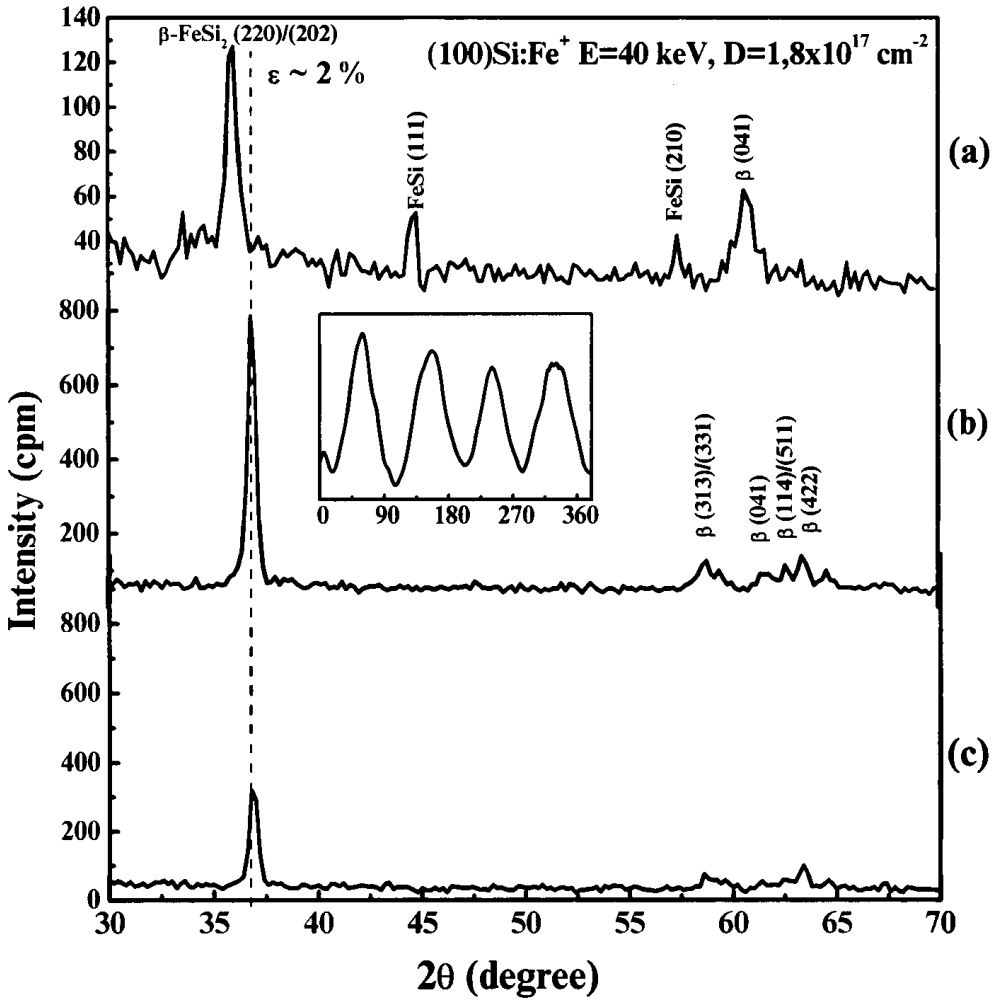


**Figure 1.** GXRD patterns for implanted Si (40 keV/1.8 × $10^{17}$ $Fe^{+}$ $cm^{-2}$): (a) after PIBT (0.75 J $cm^{-2}$); (b) after PIBT and additional TA (800 °C, 20 min); (c) after TA only (800 °C, 20 min). In the inset, the azimuth dependence of the $\beta$-$FeSi_2$ (220)/(202) diffraction peak is shown.

ratio of the integrated intensities $I_{220}$:$I_{422}$ is about 8.7 whereas for randomly oriented $\beta$-$FeSi_2$ powders this ratio is about 1.25. This indicates that the preferred grain orientation (texture) is present. In the inset of figure 1(b) the azimuth dependence of the (220)/(202) peak is shown, indicating the presence of the high degree of texture with [110] orientation on Si(100). For comparison, figure 1(c) shows the GXRD pattern of an implanted sample after TA (800 °C, 20 min) only. In this case the $\beta$-$FeSi_2$ phase is also observed, but only with the ratio of $I_{220}$:$I_{422} = 3.6$ and with a very weak texture (not shown).

### *3.2. Optical characterization*

Figure 2 shows reflectance ($R$) and transmittance ($T$) spectra of an implanted sample after PIBT and additional TA in the spectral region corresponding to the silicon substrate transparency.

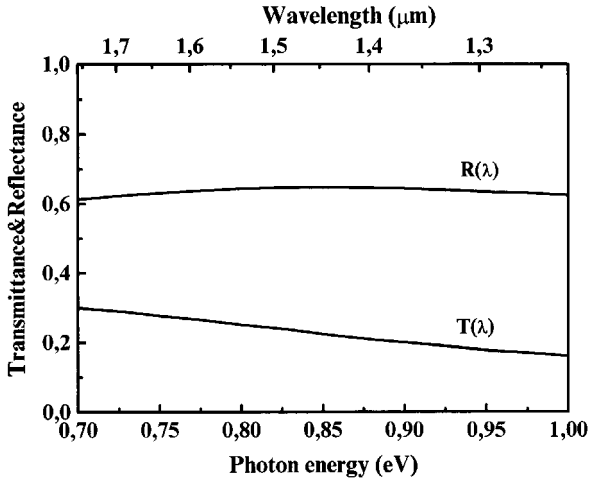


**Figure 2.** Transmittance and reflectance spectra of implanted Si (40 keV/1.8 $\times$ $10^{17}$ $Fe^{+}$ $cm^{-2}$) after PIBT (0.75 J $cm^{-2}$) with additional TA (800 °C, 20 min).

The dependence of the absorption coefficient $\alpha$ on the photon energy $E$ for the direct interband transitions is given by [24]

$$\alpha = A(E - E_g)^{1/2} \tag{1}$$

where $A$ is a constant associated with specific features of the band structure and $E_g$ is the magnitude of the direct band gap. The absorption exponent $\alpha d$ ($d$ is the layer thickness) is found according to the equation

$$\alpha d = \ln\left(\frac{1-R}{T}\right) \tag{2}$$

and from the dependence of $(\alpha d)^2$ on $E$ one can determine the $E_g$-value by extrapolating the straight line down to the intersection with the $E$-axis (figure 3). The $E_g$-value ($\sim$0.83 eV) is close to those for ion-beam-synthesized $\beta$-$FeSi_2$ given in the literature [4–6].

A substantial subgap absorption (Urbach tail) exists below the fundamental absorption edge. It appears due to the light absorption by the silicide layer defects (defect absorption) and follows the empirical rule [25]

$$\alpha = \alpha_0 \exp\left(\frac{E - E_g}{E_0}\right) \tag{3}$$

where $\alpha_0$ is a constant and $E_0$ is the inverse logarithmic slope of the Urbach tail. The parameter $E_0$ characterizes the Urbach tail width and indicates that both static structural and dynamic thermal disorders contribute to the absorption below the direct band gap. At RT, structural disorder due to the grain boundaries and their related defects has been found to make the dominant contribution to the Urbach tail [4]. The result of fitting the defect absorption to equation (3) at $E < E_g$ is shown in the inset of figure 3 by the solid line. The best-fit $E_0$-value is found to be $\sim$0.22 eV for an implanted sample subjected to PIBT and TA. The comparison of our result with literature data indicates a sufficiently high defect content in the annealed silicide layers ($E_0 \sim 0.05$ eV after TA at 900 °C for 18 h [26]). It is obvious that to decrease the $E_0$-value it is necessary to find optimal regimes of ion implantation, PIBT and TA.

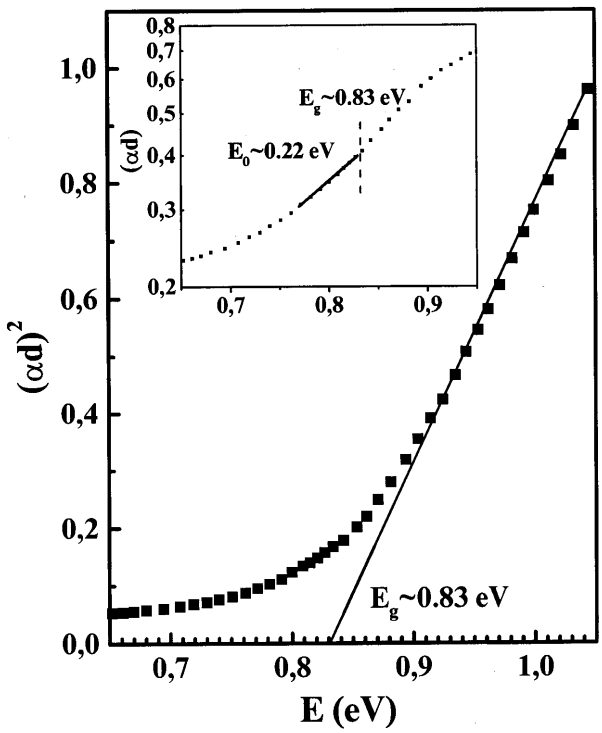


**Figure 3.** The square of the absorption exponent versus the photon energy for implanted Si after PIBT (0.75 J cm$^{-2}$) with additional TA (800 °C, 20 min). The solid line shows the extrapolation of the absorption data to determine the $E_g$-value. In the inset the spectral dependence of the absorption coefficient is shown on a log scale. The solid line is obtained from the fit to the measured data using the Urbach rule.

## 4. Conclusions

We have shown that PIBT of $Fe^+$-implanted Si leads to the formation of a mixture of two phases (FeSi and $\beta$-$FeSi_2$) with a strained state of the silicide crystal lattice. Subsequent short-duration TA (800 °C, 20 min) results in a decrease of the lattice strains and the complete transformation of the FeSi phase into $\beta$-$FeSi_2$, with the production of a highly textured layer with [110] orientation on Si(100). The results of the optical absorption measurements indicate the formation of a direct band gap structure with the optical gap $E_g \sim 0.83$ eV and with the Urbach tail width $E_0 \sim 0.22$ eV.

This work was supported by the NIOKR Foundation of Tatarstan Republic, Russian Federation (grant No 16-03), and the Russian Foundation of Basic Research (grant No 00-15-96615). The authors would like to thank V F Valeev for the ion implantation, R G Mustafin for the pulsed ion-beam treatment and V A Shustov for the x-ray measurements.

## References

[1] Bost M C and Mahan J E 1985 *J. Appl. Phys.* **58** 2696
Bost M C and Mahan J E 1988 *J. Appl. Phys.* **64** 2034
[2] Dimitriadis C A, Werner J H, Logothetidis S, Stutzmann M, Weber J and Nesper R 1990 *J. Appl. Phys.* **68** 1726

[3] Lefki K, Muret P, Cherief N and Cinti C R 1991 *J. Appl. Phys.* **69** 352
[4] Yang Z, Homewood K P, Finney M S, Harry M A and Reeson K J 1995 *J. Appl. Phys.* **78** 1958
[5] Katsumata H, Makita Y, Kobayashi N, Shibata H, Hasegawa M, Aksenov I, Kimura S, Obara A and Uekusa S 1996 *J. Appl. Phys.* **80** 5955
[6] Daraktchieva V, Baleva M, Goranova E and Angelov Ch 2000 *Vacuum* **58** 415
[7] Gumarov G G, Petukhov V Yu, Shustov V A and Khaibullin I B 1997 *Nucl. Instrum. Methods* B **127+128** 321
[8] Liu B X, Gao K Y and Zhu H N 1999 *J. Vac. Sci. Technol.* B **17** 2277
[9] Oostra D J, Vandenhoudt D E W, Bulle-Lieuwma C W T and Naburgh E P 1991 *Appl. Phys. Lett.* **59** 1737
[10] Radermacher K, Mantl S, Dieker Ch and Lüth H 1991 *Appl. Phys. Lett.* **59** 2145
[11] Reeson K J, Finney M S, Harry M A, Hutchison S V, Tan Y S, Leong D, Bearda T R, Yang Z, Curello G, Homewood K P, Gwilliam R M and Sealy B J 1995 *Nucl. Instrum. Methods* B **106** 364
[12] Reuther H and Dobler M 1996 *Appl. Phys. Lett.* **69** 3176
[13] Spinella C, Coffa S, Bongiorno C, Pannitteri S and Grimaldi M G 2000 *Appl. Phys. Lett.* **76** 173
[14] Collins C and Carlson R 1957 *Phys. Rev.* **108** 1409
[15] Kolbesen B O and Cerva H 2000 *Phys. Status Solidi* b **222** 303
[16] D'Anna E, Leggieri G and Luches A 1992 *Thin Solid Films* **218** 95
[17] Gärtner K, Götz G, Kaschner C, Kasko I, Witzmann A and Zentgraf A 1989 *Phys. Status Solidi* a **112** 747
[18] Datta A, Kal S, Basu S, Nayak M and Nath A K 1999 *J. Mater. Sci.–Mater. Electron.* **10** 627
[19] Bayazitov R M, Antonova L Kh, Khaibullin I B and Remnev G E 1998 *Nucl. Instrum. Methods* B **139** 418
[20] Hodgson R, Baglin J E E, Pal R, Neri J M and Hammer D A 1980 *Appl. Phys. Lett.* **37** 187
[21] Chen L J, Hung L S, Mayer J W, Baglin J E E, Neri J M and Hammer D A 1982 *Appl. Phys. Lett.* **40** 595
[22] Bayazitov R M, Zakirzyanova L Kh, Khaibullin I B, Isakov I F and Chachakov A F 1992 *Vacuum* **43** 619
[23] Isakov I F, Kolodii V N, Opekunov M S, Matvienko V M, Pechenkin S A and Remnev G E 1990 *Vacuum* **42** 159
[24] Pankov J J 1971 *Optical Processes in Semiconductors* (New York: Dover) p 34
[25] Urbach F 1953 *Phys. Rev.* **92** 1324
[26] Yang Z and Homewood K P 1996 *J. Appl. Phys.* **79** 4312